May 2, 1995

Final Technical Report - for NAGW-4011
5/15/94 - 2/14/95

"Palomar Observations of the Collision of Comet Shoemaker-Levy 9 with Jupiter"

G. Neugebauer, Principal Investigator
K. Matthews, A. J. Weinberger, and D. L. Shupe
California Institute of Technology

P. D. Nicholson
Cornell University

Matthews, Weinberger, Shupe and Neugebauer of the Caltech infrared astrophysics group collaborated with P. Nicholson and Cornell planetary astronomers in observing the impact of Comet Shoemaker-Levy with Jupiter using the 200-inch Telescope of the Palomar Observatory. Successful observations were obtained of all the impacts that were visible from Palomar. In addition, follow-up observations were made during the rest of July and during August, while Jupiter was still visible from the Earth.

The most significant observations are described in the enclosed two articles which have been accepted for publication in The Geophysical Research Letters.

Enclosures

To appear in the *Geophysical Research Letters*, 1995.

Palomar observations of the R impact of comet Shoemaker-Levy 9: I. Light curves

P. D. Nicholson,[1] P. J. Gierasch,[1] T. L. Hayward,[1] C. A. McGhee,[1] J. E. Moersch,[1] S. W. Squyres,[1] J. Van Cleve,[1] K. Matthews,[2] G. Neugebauer,[2] D. Shupe,[2] A. Weinberger,[2] J. W. Miles[3] and B. J. Conrath[4]

Abstract

We present near-infrared observations from Palomar observatory of the impact of fragment R of comet Shoemaker-Levy 9 with Jupiter on 21 July 1994. Two instruments were used to image the event at 3.2 and 4.5 microns simultaneously. The lightcurves from these image sequences both show two faint precursor flashes, a bright main peak, and several oscillations over the following hour. We identify the precursor flashes with the entry of the bolide into Jupiter's upper atmosphere, and with the post-impact ejecta plume rising above the planet's limb. The main peak is due to the re-entry of the collapsing plume into Jupiter's atmosphere and the resultant shock heating.

[1] Astronomy Department, Cornell University, Ithaca, New York.

[2] California Institute of Technology, Pasadena, California.

[3] National Air and Space Museum, Washington DC.

[4] NASA Goddard Space Flight Center, Greenbelt, Maryland.

Introduction

The collisions of the fragments of comet Shoemaker-Levy 9 with Jupiter in July 1994 were observed with the 5-m Hale telescope at Palomar Observatory by a joint team of astronomers from Cornell and Caltech.[1] We present here near-infrared photometric observations of the impact of fragment R. In a companion paper (Paper II) we present related mid-IR spectroscopic observations.

Observations

Palomar was well located to observe the R impact, predicted to occur at 5:26 UT on 21 July [*Chodas and Yeomans*, publicly-posted predictions, 16 July 1994]. Jupiter was at 2.34 airmasses when observations commenced at 5:19 UT, 2.5 hr after sunset. Although the sky was hazy, and conditions non-photometric by normal standards, there was no sign of cirrus or other patchy clouds. Observations ceased at 6:50 UT when the telescope reached its horizon limit, at 6.4 airmasses. The seeing at the time of the R event (at an airmass of 2.6) was estimated at 0.9″ from the size of the first flash images at 3.2 μm. Near the end of observations (at airmass 4.3), the seeing at 2.3 μm was estimated at 1.1″ from the unresolved core of the old L impact site.

Two instruments were mounted simultaneously at the Hale telescope's f/70 Cassegrain focus: the near-infrared Cassegrain camera equipped with an SBRC 256 × 256-pixel InSb array detector and a suite of broadband and circular variable filters, and Spectro-Cam 10, a mid-infrared imaging spectrometer with a Rockwell 128 × 128-pixel Si:As detector [*Hayward et al.*, 1993]. The latter instrument permitted both mid-IR imaging through seven broad-band filters between 4.5 and 12.5 μm, as well as long-slit spectroscopy in the 8–13 μm atmospheric window. The telescope's chopping secondary mirror was used to place the target area on Jupiter alternately in the field of view of each instrument, while simultaneously permitting sky background measurements in the mid-IR.

We used the near-IR camera to obtain a series of 108 individual 8 sec exposures at 3.21 μm, at intervals of ~ 30 sec, using a circular variable filter (CVF) with a bandwidth $\Delta\lambda/\lambda = 0.015$. (To avoid saturation, 20 individual 0.4 sec frames were co-added to produce each stored image.) The wavelength chosen corresponds to a region of very strong methane absorption in Jupiter's spectrum. Each image was displayed in real time, permitting the insertion of either of two neutral density filters in series with the CVF when the rapidly-brightening impact flash threatened to saturate the detector.

Simultaneously, Spectro-Cam 10 obtained a sequence of 216 nearly-continuous 10 sec images with a broadband λ3–5 μm filter, interrupted at intervals of 7–10 min to obtain low-resolution 8–13 μm spectra of the impact area.

Absolute timing was synchronized with a WWVB receiver to within ~ 0.1 sec.

Data analysis

3.2 μm images

In preliminary processing, each near-IR image was linearized, sky subtracted, flat-fielded and corrected for bad pixels. Since sky frames were taken only sporadically, the closest available sky frame was used in the reduction. A measure of the local observing conditions can be obtained from measuring the sky background signal at 3.2 μm. The background in a fixed aperture (7″ radius) for all the frames used for photometry was found to vary linearly with airmass, and the residuals from a least squares fit were less than 0.1%. If we assume that the sky background and extinction scale similarly with airmass, this linearity means that the extinction per airmass was constant over the course of the observations presented here. From this fit we derived an extinction correction of 0.10 mag/airmass for the 3.2 μm data.

The flux density from the R impact site was measured in each frame or, towards the end of observations, in the average of frame pairs. Since the shape and dimensions of the impact site changed with time, the aperture was located on the centroid of the bright spot and its size was periodically adjusted in an attempt to include all of the flux. The typical aperture radius was 2.2″. Repeating the photometry with a larger, fixed-size aperture resulted in differences of less than 1% in the measured fluxes. There was no detectable flux from the planet itself in these short exposures.

Observations of the standard star HR 8143 obtained immediately after the impact were used for absolute photometric calibration; its magnitude at 3.2 μm was taken to be 3.73 [*Neugebauer*, private

[1] Observations at the Palomar Observatory were made as part of a continuing collaborative agreement between the California Institute of Technology and Cornell University.

communication, 1994]. The attenuations due to the neutral density filters were found by measuring the difference in background between integrations made with and without the filters, and the correction was applied to the appropriate frames. The overall systematic uncertainty in the 3.2 μm fluxes is estimated to be ~6%, due mostly to calibration uncertainties.

4.5 μm images

The Spectro-Cam 10 images were reduced by first subtracting the off-Jupiter chop position frames from the on-Jupiter frames. Test images on blank sky showed that after such a subtraction there remained only a small offset that was nearly constant over the field. This offset was measured and subtracted from each Jupiter image. We registered the frames to an accuracy of about ± 1 pixel using a $\sim 90°$ arc of Jupiter's limb, and then derived an extinction of 0.24 mag/airmass from photometry of the polar cap region over the full airmass range of the data (2.37 – 5.14). We measured the total flux in a $3 \times 3''$ synthetic aperture centered on the slowly moving impact site, and calibrated the data using images of the standard star γ Aql, for which a magnitude of -0.58 at 4.8 μm was adopted [*Gezari et al.*, 1993]. The background flux from the limb of Jupiter included in the aperture, about 3 Jy, was fitted by a straight line through several of the points before the impact flashes appeared and after the site disappeared from view, and then subtracted from each data point.

The width of the 3–5 μm filter and the likelihood that the energy distribution of the impact flash is time-variable and different from that of the standard star introduce considerable uncertainty in the photometric calibration. To evaluate this problem, we calculated the responsivity of the instrument in the 3–5 μm range by dividing a low-resolution spectrum of the star μ UMa taken through this filter by a 3600 K blackbody. We then multiplied this responsivity by blackbodies of temperature 200–3000 K in order to determine the sensitivity of the effective wavelength and reddening correction to source temperature. Over the range 500–1000K, the variation in the flux calibration was found to be 10%, but lower temperatures would require a much larger correction. We have chosen a provisional correction which assumes a 500 K blackbody spectrum for the impact site, representing the middle of the range of reasonable possibilities (see Paper II). The effective wavelength is then 4.53 μm, for which the zero magnitude flux is 174 Jy. We estimate that the uncertainty in the flux calibration at this point could be as high as 20–30%.

Another source of uncertainty is the subtraction of the background flux from Jupiter in the $3 \times 3''$ synthetic aperture. This background will vary because of imperfect registration of the images and the appearance of different 5 μm features on the limb as the planet rotates. We estimate these variations to be about ± 0.5 Jy, or $\sim$ 15% of the total background, so that only the fainter parts of the light curve are significantly affected.

Lightcurves

The 3.2 and 4.5 μm lightcurves for the R impact are shown in the upper panel in Fig. 1, while the lower panel shows the initial or precursor flashes on an expanded scale. The first flash, which is temporally unresolved in our data and apparently lasted no longer than 10 sec, was observed by both instruments in frames centered at 5:34:50 (3.2 μm) and 5:34:52 UT (4.5 μm), 9 min after the predicted impact time. This first flash was followed 60 sec later by a second, much brighter flash which peaked at 5:35:48 UT, again seen simultaneously at both 3.2 and 4.5 μm. At 4.5 μm, this second flash extended over 2–3 integrations, or 20–30 sec, but the rise time may well be unresolved as the peak signal is reached in only two frames. The decay time of the second flash is quite different in the two lightcurves: $\sim$ 60 sec at 3.2 μm but $\leq$ 10 sec at 4.5 μm.

Over the following 2.5 min the impact site faded steadily at 3.2 μm but did not disappear completely. At ~5:39 UT a third, much more spectacular brightening commenced, first at 3.2 μm and slightly later at 4.5 μm. Within 6 minutes, the flux at both wavelengths had increased by a factor of $\sim$ 600 (7 mag), culminating in a broad peak at ~5:44:55 UT, 10 min after the initial flash. The peak flux occurred within 20 sec of the same time in both channels.

A slow decay in the flux at both wavelengths ensued until 5:51 or 5:52 UT, when the signal brightened again, peaking at ~5:54. This fourth peak is more pronounced at 3.2 μm where it amounts to a 45% increase in flux, than it is at 4.5 μm. (A corresponding, but weaker subsidiary peak may be visible in the IRTF lightcurves for the R impact at 7.85 μm [*Orton et al.* 1995, Fig. 7].) A fifth, rather subdued peak was observed in the 3.2 μm data at ~6:03 UT, during the acquisition of one of several low-resolution spectra by Spectro-Cam 10. There is even a hint of a sixth maximum, or more correctly a shoulder in

the declining 3.2 μm lightcurve, at ~6:14 UT. These weaker maxima occurred 9, 18 and 29 min after the main peak, suggesting a damped post-impact oscillation or 'bounce' with a period of ~ 10 min. We found no evidence for any fluctuations in sky brightness during this period which might be responsible for these signal variations, and conclude that they are real. After 6:20 UT, the signal from the R impact site became essentially undetectable at 3.2 μm, but continued to decay steadily at 4.5 μm.

Although the impact site appeared as an unresolved point source during the initial flashes, after ~6:00 UT it was clearly extended along Jupiter's limb at both 3.2 and 4.5 μm. The maximum dimension was measured at 2.1″, or ~ 8000 km at Jupiter, in agreement with the 2″ measured by *Graham et al.* [1995] at 2.3 μm. This is also comparable with the diameter of the R impact site measured on the following night at 2.3 μm, and with the diameters of medium-size impact sites seen in HST images [*Hammel et al.* 1995].

Interpretation

Our observations of the R impact are consistent with the following conceptual model, based on calculations by *Crawford et al.* [1994], *Takata et al.* [1994] and *Zahnle and MacLow* [1994] and developed in more detail by *Zahnle and MacLow* [1995]. Our interpretation is also consistent with that proposed by *Graham et al.* [1995].

We tentatively attribute the first precursor flash to thermal radiation from the bolide entering Jupiter's atmosphere, visible above the planet's limb. In the strong methane band at 3.2 μm, a vertical optical depth of unity is reached at a pressure level of $p_{3.2} \simeq$ 1 mbar [*Baines,* private communication, 1994]. The atmosphere becomes transparent to *tangential* rays at this wavelength above $p_{\rm limb} = [H/2\pi R]^{1/2} p_{3.2} \simeq$ 8 μbar, where $H \simeq$ 26 km is the atmospheric scale height in the stratosphere and $R \simeq$ 69000 km is Jupiter's radius at latitude 44°. This is at an altitude of 265 km above the 1 bar pressure level. The R impact occurred at $\theta = 4.9°$ behind the planet's limb [*Chodas and Yeomans*, publicly-posted predictions, 16 July 1994]. In order to be directly visible, therefore, the bolide must have been at an altitude of at least $z \simeq R(1 - \cos\theta) = 255$ km above the limb, or 520 km above the 1 bar level. A rough estimate of frictional heating at this altitude ($p \simeq$ 1 nbar) yields a surface temperature of ~ 2400 K, consistent with detectable emission in the near-IR.

We identify the second precursor flash with the emergence of the rising fireball, or plume, above Jupiter's limb. Using the maximum height of $h \simeq$ 3200 km measured for the A, E, G and W plumes from HST images [*Hammel et al.*, 1995], we estimate a plume ejecta velocity of $v_p = [2gh]^{1/2} = 12.5$ km/s, where $g = 2500$ cm/s^2 is Jupiter's surface gravity. For the shallowest likely penetration depth of 1 bar, and accepting the first flash as the bolide entry, the bolide's time of flight is 12 sec. Allowing for rotation of the impact site towards the limb, the plume's rise time to a height of 480 km is 38 sec. This simple picture is thus fairly consistent with the 56 sec interval between the first and second precursor flashes.

What then of the third and brightest peak? The ballistic flight time of the plume itself is $2v_p/g \simeq$ 17 min, with the last stages of re-entry corresponding roughly to the end of the main peak in near-IR emission at 5:51 UT. Although the plume material remained above the limb for many minutes after it first emerged into view, the decay of the second flash within $\leq$ 60 sec suggests either rapid expansion and adiabatic cooling of the plume, or possibly chemical changes within the plume. The plume itself therefore probably made a negligible contribution to the near-IR flux thoughout the period of the main peak [*Graham et al.*, 1995]. About 11 min after the impact, however, the center of the R impact site was carried by Jupiter's rotation onto the limb, and thus became directly visible (in thermal emission) to Earth-based observers. Moreover, at this time the bulk of plume ejecta was re-entering the jovian atmosphere, the region of fallout having reached its maximum radius of ~ 6400 km 12 min after the explosion. We therefore interpret the dramatic brightening of the impact site which began 4 min after the initial flash and peaked 6 min later to be thermal radiation from shock heating upon ejecta re-entry. In addition to fitting the observed delay of peak emission by 10 min from the impact, this scenario is consistent with the observed 8000 km extent of the impact site along the limb. Predicting the exact time evolution of the observed flux is complicated by the simultaneously varying fallout zone and viewing geometries [*Zahnle and MacLow* 1995].

Finally, we recall the oscillation with a period of 9–10 minutes which is superposed on the slow decay following the peak flux. The acoustic propagation time through Jupiter's stratosphere from the tropopause to the 0.1 mbar level is about 4 minutes. The oscil-

lation might thus be due to an acoustic or shock disturbance that moves up and down through the stratosphere prior to hydrostatic equilibration, triggered by the plume ejecta re-entry.

Acknowledgments We would like to thank the staff of the Palomar Observatory for their extra efforts on behalf of this project, which required highly unusual telescope and instrument operations. This research was supported by the NASA Planetary Astronomy Program.

References

Crawford, D., M. Boslough, T. Trucano, and A. Robinson, Numerical simulations of fireball growth and ejecta distribution during Shoemaker-Levy 9 impacts on Jupiter, *EOS, 75*, 404, 1994.

Gezari, D. Y., M. Schmitz, P. S. Pitts, and J. M. Mead, Catalog of Infrared Observations, *NASA Reference Publication 1294*, 1993.

Graham, J. R., I. de Pater, J. G. Jernigan, M. C. Liu and M. E. Brown, The fragment R collision: W. M. Keck Telescope observations of SL9, *Science, 267*, 1320-1323, 1995.

Hammel, H. B., et al., HST imaging of atmospheric phenomena created by the impact of Comet Shoemaker-Levy 9, *Science, 267*, 1288-1295, 1995.

Orton, G.S., et al., Collision of comet Shoemaker-Levy 9 with Jupiter observed by the NASA Infrared Telescope Facility, *Science, 267*, 1277-1281, 1995.

Hayward, T. L., J. W. Miles, J. R. Houck, G. E. Gull, J. Schoenwald, SpectroCam-10: A 10 micron spectrograph/camera for the Hale telescope, *Proc. SPIE , 1946*, 334-340, 1993.

Takata, T., J. D. O'Keefe, T. J. Ahrens and G. S. Orton, Comet Shoemaker–Levy 9: Impact on Jupiter and plume evolution, *Icarus, 109*, 3–19, 1994.

Zahnle, K. and M. M. Mac Low, The collision of Jupiter and comet Shoemaker–Levy 9, *Icarus, 108*, 1–17, 1994.

Zahnle, K. and M. M. Mac Low, A simple model for the light curve generated by a Shoemaker–Levy 9 impact. Preprint, 1995.

This preprint was prepared with the AGU LaTeX macros v3.1. File R1 formatted 1995 May 7.

Figure 1. (Top) R impact lightcurves from Palomar observations at 3.2 and 4.5 μm. Gaps in the 4.5 μm data indicated by the dotted curve correspond to times at which low-resolution 8–13 μm spectra were obtained. (Bottom) A detailed view of the R impact lightcurves during the first and second precursor flashes. Plotted times correspond to the mid-times of the exposures. The rms noise levels are indicated by the signal levels prior to the first flash at 5:34:50 UT. The first low-resolution spectrum was made at ~5:37 UT.

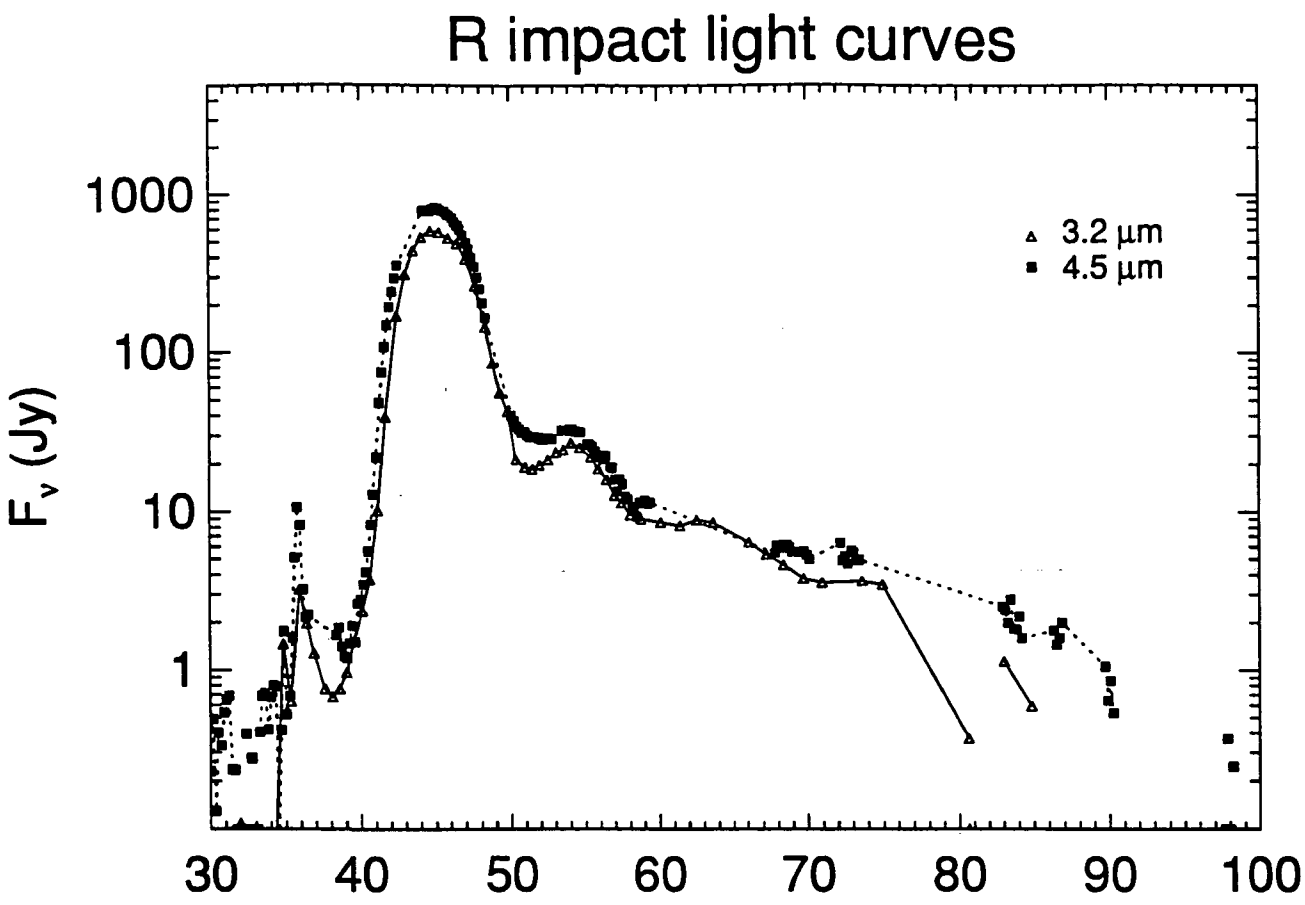
R impact light curves
1000
100
10
1
F_ν (Jy)
3.2 μm
4.5 μm
30
40
50
60
70
80
90
100

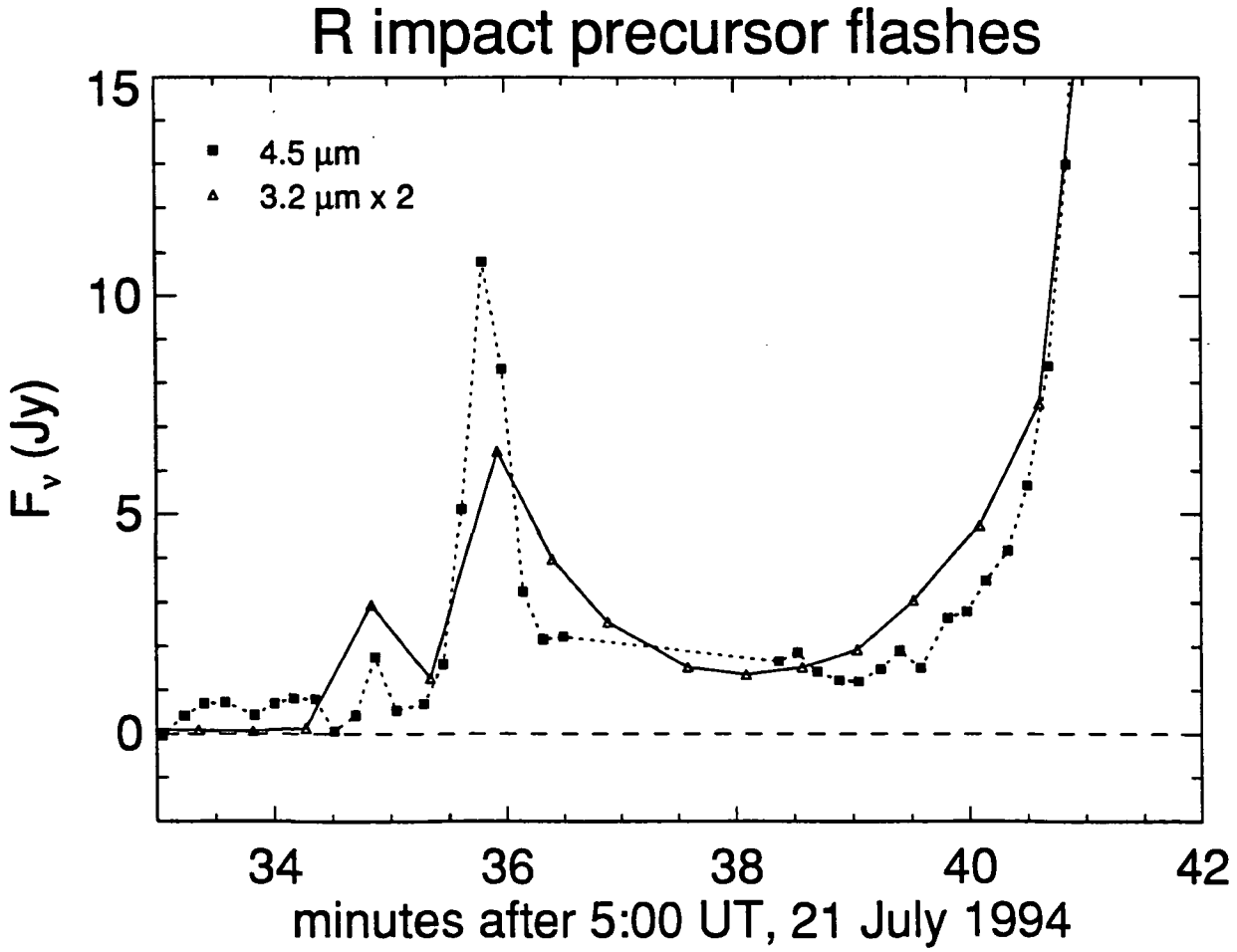
R impact precursor flashes
15
10
5
0
F_ν (Jy)
4.5 μm
3.2 μm x 2
34
36
38
40
42
minutes after 5:00 UT, 21 July 1994

To appear in the *Geophysical Research Letters*, 1995.

Palomar observations of the R impact of comet Shoemaker-Levy 9: II. Spectra

P. D. Nicholson,[1] P. J. Gierasch,[1] T. L. Hayward,[1] C. A. McGhee,[1] J. E. Moersch,[1] S. W. Squyres,[1] J. Van Cleve,[1] K. Matthews,[2] G. Neugebauer,[2] D. Shupe,[2] A. Weinberger,[2] J. W. Miles[3] and B. J. Conrath[4]

Abstract

We present mid-infrared spectroscopic observations from Palomar observatory of the impact of fragment R of comet P/Shoemaker-Levy 9 with Jupiter on 21 July 1994. Low-resolution 8–13 μm spectra taken near the peak of the lightcurve show a broad emission feature that resembles the silicate feature commonly seen in comets and the interstellar medium. We use this feature to estimate the dust content of the impact plume. The overall infrared spectral energy distribution at the time of peak brightness is consistent with emission from an optically-thin layer of small particles at ~ 600 K. Integrating over the spectrum and the lightcurve, we obtain a total radiated energy from the R impact of $\geq 2 \times 10^{25}$ ergs and a plume mass of $\geq 3 \times 10^{13}$ g.

[1] Astronomy Department, Cornell University, Ithaca, New York.

[2] California Institute of Technology, Pasadena, California.

[3] National Air and Space Museum, Washington DC.

[4] NASA Goddard Space Flight Center, Greenbelt, Maryland.

Introduction

In Paper I we described the lightcurves obtained for the R impact at Palomar at 3.2 and 4.5 μm. Here we present 8–13 μm spectra of the evolving impact site, as well as a composite spectral energy distribution at the time of peak flux.[1] The near-infrared lightcurves are also used to estimate color temperatures of the R impact precursor flashes and of the fresh impact site.

Spectroscopic observations

At intervals of 7–10 min during the course of the Palomar R impact observations, low-resolution spectra were taken in three overlapping wavelength intervals to provide complete 8–13 μm coverage with a resolution, $\lambda/\Delta\lambda \approx 100$. All spectra were obtained with a 1″-wide slit oriented parallel to Jupiter's equator and centered on the location of peak brightness measured at 4.5 μm. A total of eight complete 8–13 μm spectra were obtained, beginning at 5:37 UT and ending at 6:45 UT. The first spectrum was taken immediately following the second precursor flash, the second just prior to the peak flux at 5:45 UT, and the remainder at intervals during the decay phase. Separate spectra taken of Callisto at 1:09 UT were used for absolute flux calibration.

Data Analysis

Each 10-second exposure spectral image was reduced by subtracting the off-Jupiter chopped image and removing bad pixels by interpolation; a slight tilt was removed by 'twisting' the images so that the spectral lines were vertical in each spectral image. The wavelength scales were determined from telluric emission lines at known wavelengths in the sky frames for each wavelength segment. Because the airmass of the observations ranged from 2.65 to 5.92, extinction effects are substantial. From measurements of a region of Jupiter well away from the R impact site, we determined a wavelength-dependent extinction coefficient of 0.25–0.9 mag/airmass which was used to correct both the Jupiter and Callisto spectra for extinction effects. Except in the strong telluric ozone band between 9.3 and 9.9 μm, this procedure yielded acceptably consistent spectra.

The fluxes from both the impact site and Callisto were summed over 11 pixels (2.75″) along the slit, resulting in an effective aperture size of 2.75 × 1.0″. Although the slit did not include all the flux from Callisto, we applied no slit throughput corrections since the projected impact spot size perpendicular to the slit of $\sim$ 1.5″ was comparable to Callisto's diameter of 1.2″. The Jupiter to Callisto flux ratios were converted to absolute fluxes using the aperture photometry of *Hansen* [1976], interpolated via a blackbody model. Hansen's Callisto data were adjusted to the circumstances of July 1994 by assuming that brightness temperature scales as $r^{-\frac{1}{2}}$ and flux as Δ^{-2}, where r is the Sun-Jupiter distance and Δ is the Earth-Jupiter distance. Three of the resulting spectra are shown in Figure 1.

Results

The initial spectrum at 5:37 UT and those obtained after 6:00 UT are essentially identical, and show brightness temperatures consistent with the undisturbed jovian limb. To avoid cluttering the diagram, we have omitted spectra taken after 6:00 UT. We also plot in Fig. 1 blackbody curves for temperatures of 140, 150 and 160 K, spanning the range of undisturbed brightness temperatures expected for Jupiter in this spectral region. The absence of prominent molecular absorption or emission lines in the spectra, especially the usually strong NH_3 lines at 10.3 and 10.7 μm, may be attributable to the very high emission angle ($\geq$ 75°). The broad bump at 12 μm is due to stratospheric emission by C_2H_6, while the increase in brightness temperature towards 8 μm is due to stratospheric CH_4 emission.

Near the time of peak brightness at 3.2 and 4.5 μm, a very different 8–13 μm spectrum was observed. The three individual spectral segments, measured in succession, have been scaled in Fig. 1 to their predicted flux levels at 5:45:00 UT, the time of maximum signal at 4.5μm. This allows us to correct for the rapid changes in the absolute flux levels at this time. The scaling factors were derived from a spline fit to the 4.5 μm lightcurve, and range from 1.96 at 8–10 μm to 1.38 at 11–13 μm. Slight mismatches in the spectra in the overlap regions indicate that the uncertainties in this procedure are $\sim$15%. No distinct molecular emission features are seen in the peak spectrum, the smaller ripples being probably due to imperfections in the extinction corrections. Mid-IR spectra taken from the KAO during the R impact [*Sprague et al.*, 1994] also fail to show strong NH_3 emission lines, although

[1] Observations at the Palomar Observatory were made as part of a continuing collaborative agreement between the California Institute of Technology and Cornell University.

those of several other species are prominent.

The spectra taken at 5:49 UT have not been rescaled to a common time, and show small discontinuities due to the fading of the impact site.

Interpretation

Silicate dust emission

The 8 to 13 μm spectral slope at peak brightness is roughly matched by a Rayleigh-Jeans spectrum, suggesting a source temperature of $\geq$ 2000 K (see Fig. 1). Relative to a blackbody, however, the spectrum shows a broad emission feature between 9 and 12 μm. In spectra of T Tauri stars and star-forming regions, a 10 μm bump such as this is usually interpreted as emission from an optically-thin region of small, warm silicate grains. However, the spectrum between 8 and 9 μm is flat or slowly decreasing with wavelength, while the dust emissivity function for astronomical silicates [*Draine and Lee,* 1984] predicts that F_λ should increase with λ, even at a dust temperature, T_d, above the vaporization temperature of silicates. KAO spectra show that methane emission at 7.7 μm is prominent in the first hour after large impacts [*Sprague et al.*, 1994; *Bjoraker et al.*, 1994], and this may account for the upturn below 9 μm in our spectrum.

In the absence of detailed modelling of both atmospheric and dust components, we simply describe the non-dust component of the spectrum (presumably due to CH_4) with a power law and fit the observed F_λ to the following model:

$$F_\lambda = A_d\left[1 - \exp\left(-\tau_{9.7}Q(\lambda)/Q(9.7)\right)\right]B_\lambda(T_d) + \frac{p_0}{\lambda^n} \quad (1)$$

where $Q(\lambda)$ is the absorption efficiency, assumed to be that of interstellar silicate grains, $\tau_{9.7}$ is the dust optical depth at 9.7 μm, and A_d is the solid angle of dust emission. In the optically-thin limit, $A_d\,\tau_{9.7}$ is the total dust cross-section (in steradians) and is well-determined, although A_d and $\tau_{9.7}$ are not. The best fit to the observed spectrum is obtained for $T_d = 370$ K, $n = 7.5$, and $\tau_{9.7} \approx 0.05$, and is shown as the dotted curve in Fig. 1. The model reproduces the form of the 8–13 μm peak spectrum quite well.

Given T_d and the product $A_d\,\tau_{9.7}$, we may obtain the total mass of silicate dust:

$$M_d = \rho_d \frac{A_d \tau_{9.7} \Delta^2}{C_{9.7}} \quad (2)$$

where $\Delta = 8\times10^{13}$cm, $C_{9.7} = \frac{3}{4}Q(9.7)/a = 10^4$ cm^{-1} is the absolute volume absorption coefficient at 9.7 μm for "astronomical silicate" grains of radius $a \leq 1$ μm [*Draine and Lee* 1984], and $\rho_d = 3.3$ g/cm^3 is the assumed density of the grains. Our best fit yields a dust mass of 6×10^{12}g. This mass of dust is 20% of the total plume mass estimated below, and about 8% of the mass of a 0.5 km diameter impactor with mean density of 1.0 g/cm^3. (Note that higher dust temperatures would imply correspondingly lower values of $\tau_{9.7}$ and total dust mass; a fit with T_d = 700 K yields $M_d = 9 \times 10^{11}$ g. Larger dust particles ($a \geq 1$ μm), on the other hand, could result in a larger total dust mass being 'hidden'.)

If we multiply $A_d\tau_{9.7}$ by 17, the ratio of visible to 9.7 μm interstellar extinction in the solar neighborhood [*Roche and Aitken,* 1984], we get 1.9 square arcsec, equivalent to an optical depth of order unity for the dark impact scars seen in visible images. A silicate composition for these spots might therefore account for both their visible and mid-infrared opacities.

Color temperatures

Ideally, we might hope to determine the evolving temperature of the impact site from the ratio of 3.2 to 4.5 μm fluxes shown in Fig. 1 of Paper I. However, the emission may well be optically thin, and dominated in the near-IR by molecular emission bands. This is especially likely to be the case at 3.2 μm, which is a region of strong methane absorption. Subject to this caveat, we have attempted to calculate color temperatures for the precursor flashes, using the measured peak fluxes at 3.2 and 4.5 μm from Fig. 1 as well as the corresponding fluxes at 2.3 μm measured by *Graham et al.*, [1995]. For the first (bolide entry?) flash, we find a consistent color temperature of 1000$\pm$120 K.

The peak of the second flash (the rising plume) gives an unexpectedly low 630$\pm$50 K, perhaps because the plume is seen at this time through a significant line-of-sight optical depth of methane. However at 5:36:30 UT, with the plume 20 scale heights higher and thus above sensible atmospheric absorption, we find a color temperature of 950 $\pm$ 150 K. This may represent the true plume temperature $\sim$ 90 sec after the impact. Two minutes later we find $T_{col} = 820 \pm 100$ K.

During the growth and decay of the main peak, we find that the color temperature of the R impact site remains relatively constant, varying from a minimum of 600 K at 5:41 UT to a maximum of 1150 K

at 5:48 UT. The average color temperature between 5:44 and 6:10 UT is ~1000 K. Although the actual temperatures may differ, the 3.2/4.5 μm flux ratio is strikingly constant over a period in which the absolute fluxes vary by a factor of a hundred. This uniformity of temperature is a strong argument in favor of our interpretation in Paper I that the main flux peak is due to emission from shock-heated re-entering ejecta, rather than from the plume itself, which is predicted to cool rapidly to space [*Zahnle and MacLow*, 1995].

Figure 2 shows a composite spectrum of the R impact at the time of peak flux (5:45 UT), including the 8–13 μm spectrum from Fig. 1, the peak fluxes at 3.2 and 4.5 μm from Fig. 1 of Paper I, and the corresponding peak flux at 2.3 μm measured by *Graham et al.*, [1995]. (Also shown for comparison is the low-resolution spectrum acquired immediately after the precursor flashes at 5:37 UT, scaled to a 1″ square solid angle.) It is impossible to fit all three near-IR points with a single blackbody; the range of plausible temperatures is indicated by the 550 K and 1000 K blackbody spectra fitted to the 2.3/3.2 and 3.2/4.5 μm flux ratios, respectively.

A simple model which at least approximately fits all of the measurements — and is also more physically plausible than pure blackbody emission — consists of a dusty, optically-thin emitting region with a temperature of ~ 600 K and an emissivity which scales as λ^{-1}. The latter is consistent with emission by small solid grains with radii $r \ll \lambda$ and constant refractive index [*van de Hulst*, 1957], and is suggested by the silicate dust fit to the 8–13 μm spectrum in Fig. 1. Such a model is shown as the dot-dashed curve in Fig. 2, fitted approximately to the near-IR points. The deviations of the observed fluxes from the model may be due to CH_4 and silicate emission. The model implies an emissivity-optical depth product of $\epsilon\tau \simeq 0.022$ at 4.5 μm and 0.010 at 10 μm, for an assumed source solid angle of 1 square arcsec. A similar optical depth in stratospheric haze particles at 10 μm is implied by our preliminary analyses of high-resolution spectra of the cooling impact sites in the 8–10 μm region [*Gierasch et al.*, 1994].

Energetics and plume mass

Given a model of the spectrum of the peak emission from the R impact site, and the observed constancy of color temperature during the main peak, we may use the measured 3.2 μm lightcurve in Fig. 1 of Paper I to estimate the total energy radiated by the impact site in the near- to mid-IR region. We adopt the 600 K dust emission model, for which the ratio η of the bolometric flux to F_λ at 3.2 μm is 6.03 μm.[2] Making the further assumption of an isotropic radiator, the total radiated energy is then given by

$$E = \frac{4\pi\Delta^2\eta c}{\lambda^2} \int F_\nu dt. \qquad (3)$$

We find a total radiated energy of $\geq 2.2 \times 10^{25}$ ergs, or 2% of the total kinetic energy of a 0.5-km diameter icy comet impacting Jupiter at 60 km/s. This estimate is probably a lower limit because of (i) the emission which occurs during the first ~ 40 sec when the fireball is behind the limb, and (ii) possible preferential emission in a direction away from the Earth. Probably the biggest unknown in this calculation is the uncertain geometry of the impact site. *Zahnle and MacLow* [1995] have taken the first steps towards a more realistic model of the observed lightcurve.

Note that essentially all of this energy is received from the shock-heated re-entry phase; the flashes due to the bolide and plume, as interpreted in Paper I, contribute a negligible fraction of the total radiated energy. Equating the radiated energy to the kinetic energy of the descending plume, for an assumed vertical re-entry velocity of 12.5 km/s, we obtain a lower limit to the total plume mass of 3×10^{13} g.

Acknowledgments We would like to thank the staff of Palomar Observatory for their extra efforts on behalf of this project, which required unusual telescope and instrument operations. James Graham and Imke dePater generously provided advance copies of the Keck lightcurve, from which the 2.3 μm points in Fig. 2 were taken. This research was supported by the NASA Planetary Astronomy Program.

[2] For a λ^{-1} emissivity, η reaches a minimum of 3.75 at 900 K, and then increases to 6.1 at 1500 K.

References

Bjoraker, G., T. Herter, G. Gull, S. Stolovy and B. Pirger, Detection of water in the fireball of fragments G and K of Comet Shoemaker–Levy 9, paper presented at Division of Planetary Sciences meeting, Amer. Astro. Soc., Washington DC, Oct 31, 1994.

Draine, B. T. and H. M. Lee, Optical properties of interstellar graphite and silicate grains, *Astrophys. J., 285*, 89–108, 1984.

Gierasch, P. J., J. Goodman, T. Hayward, C. McGhee, J. Moersch, P. Nicholson, S. Squyres, J. Van Cleve, K. Matthews, G. Neugebauer, G. Bjoraker, B. Conrath and G. Orton, A physical interpretation of the SL–9 impacts observed from Palomar, paper presented at Division of Planetary Sciences meeting, Amer. Astro. Soc., Washington DC, Oct 31, 1994.

Graham, J. R., I. de Pater, J. G. Jernigan, M. C. Liu and M. E. Brown, The fragment R collision: W. M. Keck Telescope observations of SL9, *Science, 267*, 1320-1323, 1995.

Hansen, O. L., Thermal emission spectra of 24 asteroids and the Galilean satellites, *Icarus, 27*, 463–471, 1976.

Roche, P. F. and D. K. Aitken, An investigation of the interstellar extinction. I. Towards dusty WC Wolf–Rayet stars, *Mon. Not. R. Astron. Soc., 208*, 481–492, 1984.

Sprague, A. L., D. M. Hunten, F. C. Witteborn, R. W. H. Kozlowski, D. H. Wooden and G. Bjoraker, KAO observations of Jupiter during and following the impact of Comet SL-9 fragments R and W using HIFOGS (4.9–9.4 and 9.3–14.5 μ), paper presented at Division of Planetary Sciences meeting, Amer. Astro. Soc., Washington DC, Oct 31, 1994.

van de Hulst, H. C. *Light Scattering by Small Particles,* 470 pp., Wiley, New York, 1957. Reprinted by Dover, New York, 1981.

Zahnle, K. and M. M. Mac Low, A simple model for the light curve generated by a Shoemaker–Levy 9 impact, preprint, 1995.

This preprint was prepared with the AGU LaTeX macros v3.1. File R2 formatted 1995 May 7.

Figure 1. Low-resolution ($\lambda/\Delta\lambda = 100$) spectra obtained immediately after the second flash (5:37 UT) and before any significant brightening of the R impact site at 10 μm; just prior to the peak brightness of the third flash (5:43 UT); and during the decay phase (5:49 UT). The region of telluric ozone absorption is blanked out by the vertical grey bar. The three segments of the peak spectrum have been separately scaled to the predicted peak fluxes at 5:45 UT, as described in the text. The dotted curve shows the model of silicate dust emission fitted to the peak spectrum (see text), while the dashed curve represents a 2000 K blackbody. Dot-dashed curves show blackbody spectra at characteristic undisturbed jovian temperatures of 140, 150 and 160 K.

Figure 2. Composite spectrum of the R impact at the time of maximum flux (5:45 UT). Near-IR data are from Fig. 1 of Paper I and from *Graham et al.* [1995] (at 2.3 μm), and the mid-IR spectrum is from Fig. 1. The dot-dashed curve is the 600 K λ^{-1} small-particle haze model fitted to the 2.3, 3.2 and 4.5 μm fluxes, while the dashed curves show blackbody spectra which bracket the near-IR points. The pre-impact 8–13 μm spectrum is included for comparison, along with 140 and 160 K blackbodies. All model spectra assume a 1 square arcsec solid angle.

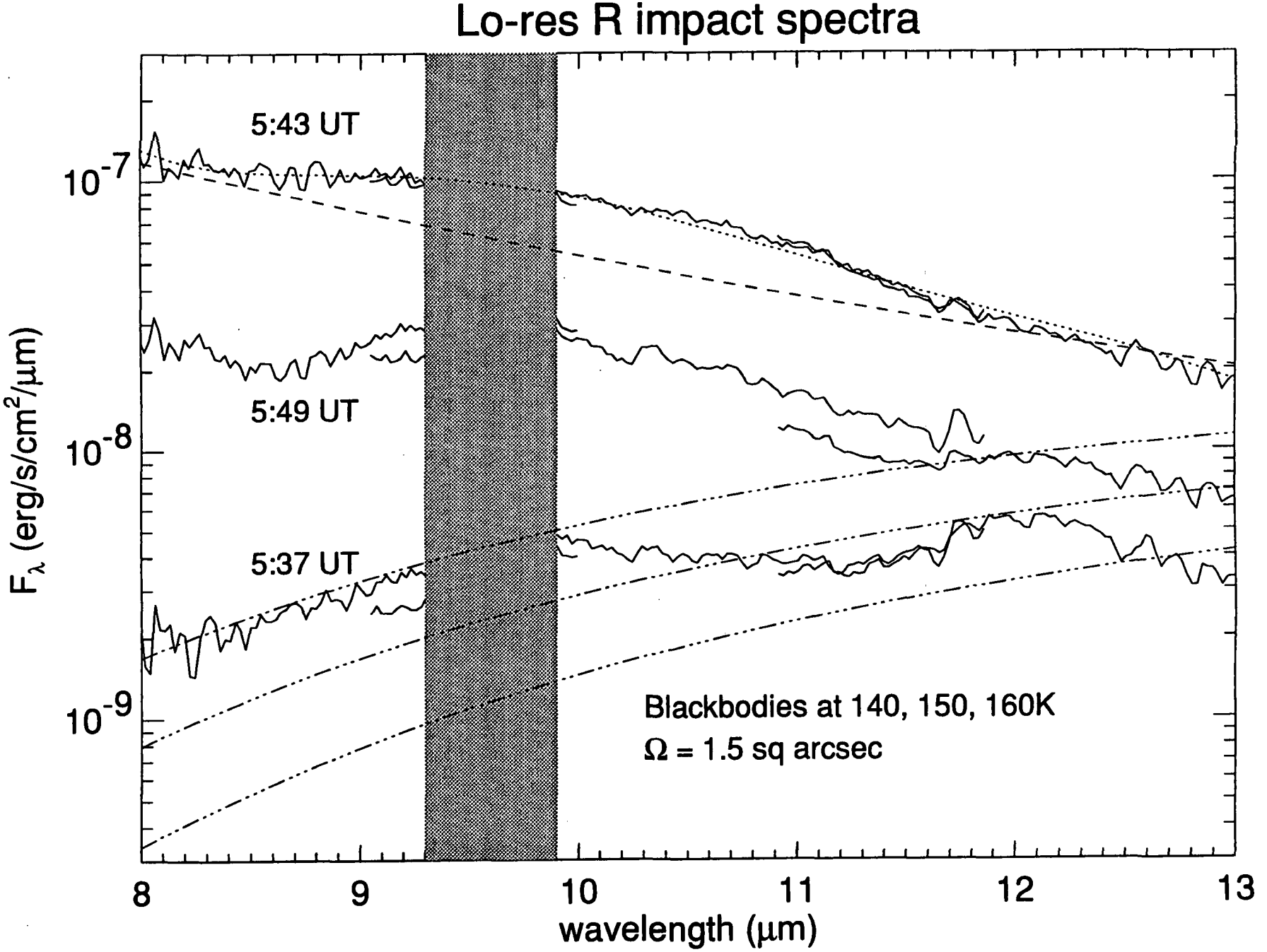
Lo-res R impact spectra
5:43 UT
5:49 UT
5:37 UT
10^{-7}
10^{-8}
10^{-9}
F_λ (erg/s/cm^2/μm)
Blackbodies at 140, 150, 160K
Ω = 1.5 sq arcsec
8
9
10
11
12
13
wavelength (μm)

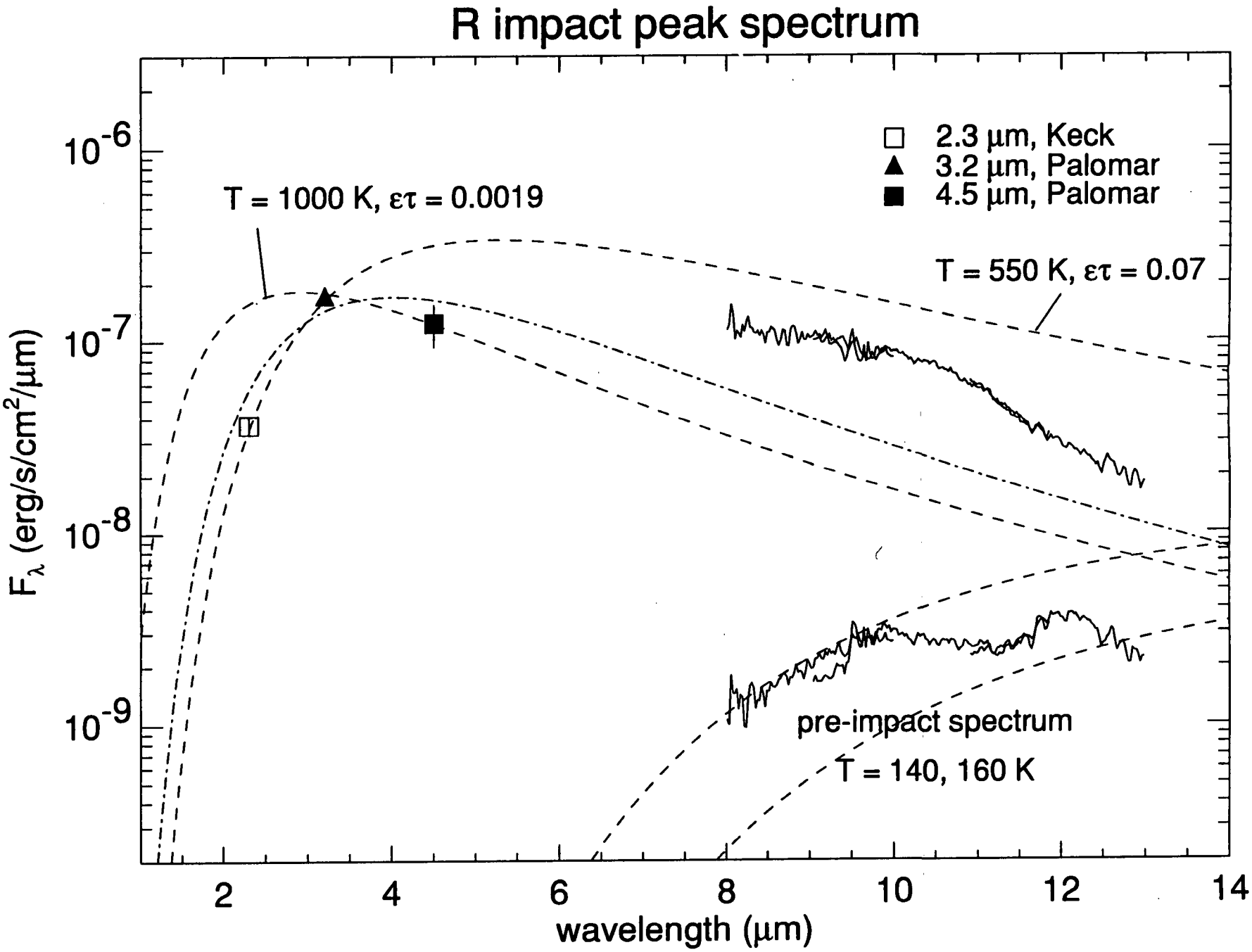
R impact peak spectrum
2.3 μm, Keck
3.2 μm, Palomar
4.5 μm, Palomar
T = 1000 K, ετ = 0.0019
T = 550 K, ετ = 0.07
pre-impact spectrum
T = 140, 160 K
F_λ (erg/s/cm^2/μm)
wavelength (μm)
10^{-6}
10^{-7}
10^{-8}
10^{-9}
2
4
6
8
10
12
14